MODEL-BASED PLANNING OF SENSOR PLACEMENT AND OPTICAL SETTINGS

Kostantinos Tarabanis

Department of Computer Science
Columbia University
New York, New York 10027

Roger Y. Tsai

IBM T.J. Watson Research Center
Manufacturing Research
Yorktown Heights, New York 10598

Abstract

We present a model-based vision system that automatically plans the placement and optical settings of vision sensors in order to meet certain generic task requirements common to most industrial machine vision applications. From the planned viewpoints, features of interest on an object will satisfy particular constraints in the image. In this work, the vision sensor is a CCD camera equipped with a programmable lens (i.e. zoom lens) and the image constraints considered are: visibility, resolution and field of view. The proposed approach uses a geometric model of the object as well as a model of the sensor, in order to reason about the task and the environment. The sensor planning system then computes the regions in space as well as the optical settings that satisfy each of the constraints separately. These results are finally combined to generate acceptable viewing locations and optical settings satisfying all constraints simultaneously. Camera planning experiments are described in which a robot-arm positions the camera at a computed location and the planned optical settings are set automatically. The corresponding scenes from the candidate viewpoints are shown demonstrating that the constraints are indeed satisfied. Other constraints, such as depth of focus, as well as other vision sensors can also be considered resulting in a fully integrated sensor planning system.

CONTENTS

List of Illustrations

1.1 Introduction

Most current machine vision applications operate in environments that have been laboriously set up. The location of the sensors along with their settings, the lighting arrangement, the position and orientation of each object in the workspace have all been carefully chosen so that the task at hand can be performed successfully. When errors (e.g. robot inaccuracy) alter the environment these parameter settings can potentially become unsatisfactory.

Consequently, these applications have limited intelligence and flexibility. This is the case despite the fact that there is information available that can be used to generate strategies to *plan* many task parameters (Ref. 11). For instance, the geometric and physical information, that is often available today in manufacturing in the form of CAD/CAM models of parts as well as sensor models, can be used to automatically generate sensor and illuminator placement strategies for tasks involving these parts, such as inspection and gaging. In general, this can lead to an integrated manufacturing environment that would also operate more flexibly and more autonomously as various processes can be planned and performed automatically.

In this paper, we present methods to plan camera placement and optical settings so that the features of interest are:

- visible,

- contained entirely in the sensor field of view and

- resolved by the sensor to a given specification.

An outline is given of each planning technique. Results are then presented for actual camera planning in a robotic workcell at poses and optical settings at which a given visual target can be viewed satisfying all the previous constraints, thus demonstrating the effectiveness of the method.

1.2 Visibility Planning

In the sensor placement planning problem, the domain of feasible sensor locations is firstly limited to regions in three-dimensional space from where the feature to be observed is *visible*. This visibility domain is further restricted to locations where other task requirements (i.e. resolution, field of view) can be satisfied. In this section, we will overview an algorithm that generates regions in three-dimensional space from where a given convex polygonal visual target can be viewed in its entirety without being obstructed by occluding polyhedral objects. The details of this algorithm can found in Ref. 3.

1.2.1 Outline of the Visibility Planning Algorithm

The visibility planning algorithm first considers the faces of the occluding polyhedron as occluding polygons. It then decomposes the problem of determining occlusion-free regions in space for a general occluding polygon and a convex target polygon into similar subtasks between convex polygons. The two decompositions introduced for this purpose, along with the method to solve the convex subproblems, are briefly described in the next sections. The occluded regions of the faces of the polyhedron are then unioned to generate the occluded region of the polyhedron as a whole. The complement of the occluded region is the visibility region, from where the entire target can be viewed.

1.2.1.1 Material-Hole Decomposition (Loop Decomposition)

Figure 1 shows an occluding polygon with a hole in it. The occluded region for viewing a target T with an occluding polygon B containing a hole H in it is equal to the occluded region caused by B (shown in Figure 2) less the region in space where the camera can view the target T through the hole H (shown in Figure 3). The first subtask is to determine the occluded region caused by the *material* polygon B. The second subtask is to determine the viewing region through the hole H. The resultant occluded region is equal to the difference of the above two regions, shown in Figure 4. In general, the following formula holds:

$$Occluded\ Region_{resultant} = Occluded\ Region_{material} - Viewing Region_{hole\ within\ material} \qquad (1)$$

However, two levels of decomposition are actually needed to accomplish the task in general. If the occluding polygon B or the hole H within B or the target T are not convex, then the two subtasks are still not convex, and therefore, another level of decomposition is needed, as shown in the next section.

1.2.1.2 Convex Material-Gulf Decomposition (Convex Decomposition)

Consider the situation in Figure 1 discussed earlier. Suppose that the occluding polygon B is not convex but is shaped like that in Figure 5. Then it is necessary to decompose B into its convex hull B_{hull} and a gulf B_{gulf} such that

$$Polygon = Convex\ Hull - Gulfs \qquad or \qquad B = B_{hull} - B_{gulf} \qquad (2)$$

The resultant occluded region is equal to the difference of the occluded region of the convex hull less the viewing region of the gulf. However, to obtain the correct viewing region, the gulf should be enlarged to become B_{equiv_hole} , a hole that is equivalent to the gulf in this viewing relation as shown in Figure 6. The algorithm for the construction of the equivalent hole can be found in Ref. 3. The equivalent hole shown in Figure 6 is concave and must be decomposed itself into convex parts in a similar fashion. The resultant viewing region through the gulf is shown in Figure 7, and the resultant occluded region is shown in Figure 8.

1.2.1.3 Convex Visibility Planning

After the above two decompositions (loop and convex), what remains is the basic convex visibility planning task. There are two kinds of convex tasks,

- Occluded region computation,

  where a convex polygon occludes a convex target, and

- Viewing region computation,

  where a convex target can be viewed through a convex hole.

The occluded region is bounded by a family of limiting separating planes defined by edge-vertex or edge-edge pairs from the occluding and target polygons such that the entire target and occluding polygons are placed in different half-spaces (Figure 2). On the other hand, the viewing region is bounded by a family of limiting separating planes defined by an edge on the hole polygon and a vertex or edge on the target polygon such that the entire target and hole polygons are placed in the same half-space (Figure 3). Both regions can be computed efficiently (Ref. 3) and then be combined to construct the occluded region of the general occluding polygon and target.

1.3 Resolution Planning

In many automatic inspection tasks, it is required that a unit feature size on an object appear as a minimum number of picture elements on a sensor. This resolution constraint can be satisfied by properly selecting the image sensor, as well as by carefully planning its placement and settings. In this section, we shall present a method to plan the latter two, namely, the camera location and the optical settings of a lens, so that chosen features can be resolved to meet a given specification.

1.3.1 Outline of the Resolution Planning Method

Customarily, the limiting resolution is specified as the minimum number of picture elements on a sensor per unit length in object space. The objective of resolution planning is to determine the sensor parameters that achieve this resolution.

Consider the minimum feature size shown in Figure 9 as the incremental length l on the line segment AB, as well as its image w. The goal is to determine $D = f_1(w,l,f)$ and $d = f_2(w,l,f)$ that satisfy the resolution constraint for the sensor, where D is the distance of the front nodal point, FNP, of the lens to the line segment AB, d is the effective focal length, namely the distance of the back nodal point, BNP, of the lens to the image plane, f is the intrinsic focal length of the lens, that is, the focal length of the lens for an object at infinity, l is the minimum feature size to be resolved, w is the length of l in the image plane and f_1, f_2 are the functional relationships to be determined.

The existing approach to this problem (Ref. 1) involves an iterative procedure to estimate the object and image distances D and d that satisfy the resolution constraint. In the following, we will present a *direct* method to compute D and d that meet the resolution requirement. In addition, a technique is described that determines the object distance D as well the optical settings of a variable focal length lens that again satisfy the resolution constraint.

Resolution planning for a constant intrinsic focal length lens

In Figure 9, when AB is viewed orthogonally the following relationships hold:

$$\frac{1}{D} + \frac{1}{d} = \frac{1}{f} \tag{3a}$$

$$\frac{d}{D} = \frac{w}{l} \tag{3b}$$

Equation (3a) is the Gaussian lens law applied to a general coaxial optical system with D and d measured from the principal planes in the object and image spaces respectively. On the other hand, equation (3b) expresses the linear magnification of the minimum feature l. By combining (3a) and (3b) the object and image distances D and d can be directly computed from the following relationships:

$$D = (1 + \frac{l}{w})f \tag{4a}$$

$$d = (1 + \frac{w}{l})f \tag{4b}$$

Consequently, given the resolution requirement w/l and the intrinsic focal length f of the lens, the object and image distances D and d that satisfy the resolution constraint in the limit can be determined from (4a) and (4b) respectively. For object distances smaller than the value of D computed from (4a) and their respective conjugate image distances, $d/D > w/l$ and therefore the resolution requirement is clearly satisfied.

In all the previous relationships, the length w of the image of the minimum feature is expressed in the sensor plane. However, when the limiting resolution is specified as the minimum number of picture elements in the frame buffer required to resolve l, then the scale factor that relates the sensor element spacing of the CCD array to the pixel element spacing of the frame buffer must be known (Ref. 8) in order to compute w.

Resolution planning for a variable intrinsic focal length lens

Previously for a constant intrinsic focal length lens, f is fixed and thus the object and image distances D and d computed from (4a) and (4b) respectively, are unique. For a variable focal length lens, f varies and can be set as desired. In this case, D and d can assume a range of values from (4a) and (4b) limited only by the working range of the specific lens.

In order to achieve for a given variable focal length lens these planned values of D, d and f according to (4a) and (4b), a mapping needs to be established between the parameters to be planned (D, d and f) and the lens parameters that can be controlled (e.g. zoom and focus settings). This mapping between the two parameter spaces is determined from the *calibration* of the programmable lens. Camera calibration techniques provide both the optical characteristics of the lens (i.e. intrinsic parameters such as the effective focal length d) as well as the 3D position and orientation of the camera frame relative to a certain world coordinate system (i.e. extrinsic parameters such as the object distance D). Therefore, by performing calibration at different optical settings of the programmable lens, this mapping can be determined, and thus the planned parameters can be set.

1.3.1.1 Programmable lens calibration

In this section, we present the programmable lens calibration technique that determines the mapping between the lens parameters D, d and f, and the controllable settings of the lens, which in our case are the zoom and focus functions. This mapping is required for both resolution planning (see previous section), as well as field of view planning (see "Field of View planning of a variable intrinsic focal length lens"). The technique described here has more general applications however, since programmable lens calibration is needed in many machine vision applications that employ such lenses for their versatility.

This mapping between the planned parameters D, d and f, and the lens control parameters can be described by the following relationships:

$$D = g_1(z_s, f_s, ...) \tag{5a}$$

$$d = g_2(z_s, f_s, ...) \tag{5b}$$

$$f = g_3(z_s, f_s, ...) \tag{5c}$$

where g_1, g_2 and g_3 are the mappings to be determined and z_s and f_s are the zoom and focus settings respectively. These relationships (5a),(5b) and (5c) can be established by calculating the intrinsic parameters of the programmable lens as well as the extrinsic parameters of the camera pose (Ref. 9) at sampled zoom and focus settings while interpolating at other settings.

When performing calibration at the sampled optical settings, the camera is positioned to view a coplanar set of calibration points at the sharpest focus. The camera to object distance that achieves the sharpest focus is found by using an autofocusing scheme which is described in the next section. The calibration procedure computes, among

other things, the object distance D and the effective focal length d of the lens, which are needed in (5a) and (5b) respectively. The results of the calibration for our lens are shown in Figure 11 and Figure 12, where the magnification ratio d/D and the object distance D for our zoom lens are plotted as a function of the zoom and focus settings. It should be noted that the ratio d/D was found in calibration to be generally more stable than either d or D alone and was therefore substituted for the image distance d as a parameter to be planned.

At this point, given the resolution requirement and the calibration of the programmable lens, (4a), (4b) (or (3b)), (5a) and (5b) can be combined to determine the object distances as well as the associated lens optical settings that satisfy the resolution constraint.

Autofocusing scheme: The camera to object distance yielding the sharpest focus of the image is determined by a simple autofocusing scheme in which the camera is placed at systematically increasing distances away from a calibration pattern while the quality of focus of the image is measured at each distance. The camera is mounted on a robot manipulator and moved incrementally away from the calibration pattern. At each position a focus quality criterion in a window of the image is evaluated. The values of the criterion should monotonically increase to a maximum at the distance of sharpest focus.

The focus quality criterion used is the thresholded gradient magnitude scheme (Ref. 12), which estimates the gradient of the image intensity at each image point and sums all the magnitudes greater than a threshold value. We employed this criterion with no threshold on an image that contains a high contrast circular disk. A ring around the disk periphery was chosen as the evaluation window for the image gradient computations since this is the region where the edge characteristics are affected by the focus quality. This window typically contained about 800 pixels and was automatically detected in the experiments.

In the longer focal length range of the zoom lens, the depth of field is smaller and therefore the camera to object distance yielding the sharpest focus of the image could be easily determined. However, in the shorter focal length range, the gradient magnitude values gave no clear peak unless the aperture was fully open to reduce the depth of field. The aperture can indeed be opened in the shorter focal length range without affecting the distance of sharpest focus (Ref. 12).

1.4 Field of View Planning

In the first section where occlusion-free regions for a visual target were computed, it was implicitly assumed that there were no field of view limitations. In other words, the sensor had a 180 degree view angle and therefore orientation of the sensor was immaterial. In this section, we shall address the field of view constraint and thus plan sensor location and optical settings so that the feature is totally within the sensor limited field of view.

1.4.1 Outline of the Field of View Planning Method

For a CCD camera, the field of view is limited by the minimum dimension corresponding to the active sensor area in the image plane. Any observed feature must project onto the image plane with a length at most equal to this minimum dimension, otherwise it will be truncated at some orientation of the optical axis.

Consider a line segment AB of length L with an image of length W, both shown in Figure 10. The goal is to determine $D = h_1(W,L,f)$ and $d = h_2(W,L,f)$ that satisfy the field of view constraint for the sensor, where D is the distance of the front nodal point, FNP, of the lens to the line segment AB, d is the effective focal length, namely the distance

5

of of the back nodal point, BNP, of the lens to the image plane, f is the intrinsic focal length of the lens, L is the size of the feature that must be inside the sensor field of view, W is the length of L in the image plane and h_1, h_2 are the functional relationships to be determined.

The existing approach to this problem (Ref. 1) again involves an iterative procedure to estimate the object and image distances D and d that satisfy the field of view constraint. In the following, a *direct* method to compute D and d that meet the field of view requirement is presented, as well as a technique that determines the object distance D along with the optical settings of a variable focal length lens that again satisfy the field of view constraint.

Field of View planning for a constant intrinsic focal length lens

In Figure 10, when AB is viewed orthogonally the following relationships hold:

$$\frac{1}{D} + \frac{1}{d} = \frac{1}{f} \qquad (7a)$$

$$\frac{d}{D} = \frac{W}{L} \qquad (7b)$$

Equations (7a) and (7b) are the Gaussian lens law and the magnification relationship, similar to (3a) and (3b) respectively.

Consider the case where the optical axis passes through the midpoint M of AB. In this case W can be at most equal to the minimum image plane dimension, I_{min} (in any other case, W is constrained to be even smaller). Therefore, the right-hand side of (7b) in the field of view limit becomes I_{min}/L defining as a result a maximum magnification ratio:

$$\frac{d}{D} = \frac{I_{min}}{L} \qquad (7c)$$

By combining (7a) and (7c), the object and image distances D and d can be directly computed from the following relationships:

$$D = (1 + \frac{L}{I_{min}})f \qquad (8a)$$

$$d = (1 + \frac{I_{min}}{L})f \qquad (8b)$$

Consequently, given the field of view requirement I_{min}/L and the intrinsic focal length f of the lens, the object and image distances D and d can be determined from (8a) and (8b) so that the field of view constraint is satisfied in the limit. For object distances larger than the value of D computed from (4a) and their respective conjugate image distances, $d/D < I_{min}/L$ and therefore the field of view requirement is clearly satisfied.

Field of View planning for a variable intrinsic focal length lens

Similar to resolution planning for a variable intrinsic focal length lens, (8a) and (8b) now define a range of values for D and d since the intrinsic focal length f of the lens can vary.

In order to achieve for a given variable focal length lens these planned values of D, d and f according to (8a) and (8b), the mapping given by (5a-c) between the parameters D, d and f and the lens parameters that can be controlled is again needed. As was described in "Resolution Planning", (5a),(5b) and (5c) can be established from calibration of the programmable lens.

Consequently, given the maximum magnification ratio I_{min}/L and the lens calibration, relationships (8a), (8b) (or (7b)), (5a) and (5b) can be combined to determine the object distances as well as the associated lens optical settings that satisfy the field of view constraint so that the line segment AB is not truncated by the field of view cone of the camera.

1.5 Test Results

A working system for visibility, resolution and field of view planning has been implemented. In this section, we seek to demonstrate that the results produced by the working system, which incorporates the new method, are correct.

1.5.1 Setup Description

The visibility algorithm was implemented in AML/X, an object-oriented programming language intended for use in design and manufacturing applications. The programs are run in the TGMS (Tiered Geometric Modeling System) environment (Ref. 5). TGMS provides an object-oriented programming interface to our in-house solid modeling system, GDP (Geometric Design Processor) (Ref. 6), as well as many geometry classes and methods. In this framework, the occluding and target objects as well as the viewing and occluded regions are represented as solids and any operations on them (e.g. convex hull, boolean set operations) are conveniently developed.

The experimental setup is shown in Figure 14. A Javelin CCD 480 x 384 camera is fastened to the last joint of an IBM Clean Room Robot (CRR). The CRR has two manipulators, each with seven joints, which consist of three linear joints (x,y,z), three rotary joints (roll, pitch and yaw) and the gripper joint.

A Vicon zoom lens with two close-up lenses or diopters (4-diopter and 2-diopter, making it a 6-diopter) is mounted on the CCD camera. The zoom lens has three motorized functions: zoom, focus and iris. For zoom and focus, potentiometers provide feedback of the lens element position. The zoom ratio of the lens is 6X with a focal length range of 12.5-75 mm (without the 6 diopter close-up lenses).

The occluding object and the target are shown as CAD models in Figure 15. The target to be viewed is part of the occluding object itself, namely the top face T of the enclosed cube. Figure 13 shows the actual object and target used in the real camera placement experiments. This object is assembled from smaller primitive objects (i.e. cubes, parallelpipeds etc.) so that it can be reconfigured to test a variety of occlusion arrangements.

1.5.2 Experimental Procedure

A three-dimensional solid model of the occluding object and the target is built in our geometric modelling system and the occluded region associated with the chosen target is generated by the visibility algorithm. Specifically, the occluding object is first decomposed into faces. Then, each face that lies "above" the target (i.e. in the half-space defined by the target and the outward pointing normal to the target) is treated as a separate occluding polygon. The union of the occluded regions of all faces of the object that lie above the target produces the final occluded region.

After the occluded region is determined, viewing positions inside the visibility regions are computed that satisfy the resolution and field of view constraint.

In the case of a fixed focal length lens, the resolution requirement generates an upper bound for the object distance D that can be computed from (4a), while conversely, the field of view constraint produces a lower bound for D determined by (8a). Consequently, values for the object distance can be chosen between these bounds and inside the visibility regions. The associated image distance d can then be computed from the Gaussian lens equation knowing D and f. In this manner all three constraints are satisfied simultaneously.

For the case of a variable focal length lens, the magnification ratio d/D is chosen to be greater than the given resolution limit w/l, but less than the field of view limit I_{min}/L. From the programmable lens calibration (Figure 18), this range of d/D determines at first an admissible domain of zoom and focus settings and consequently (Figure 12) an admissible range for the object distance D. The optical settings are then set and the camera is positioned inside the visibility region at a distance D away from the feature, where D is inside this admissible range.

For both the constant as well as the variable intrinsic focal length cases, the orientation of the camera is such that the feature is viewed orthogonally and the optical axis passes through the midpoint of the feature.

The manipulator with the mounted camera is used to place the camera at the chosen viewing positions with respect to the occluding object and target. Each camera position chosen is known only with respect to an object coordinate system. What needs to be determined is the manipulator location that places the camera at the chosen position. This manipulator location can be computed from the hand-eye relationship (Ref. 10) and the pose of the object in the robot world coordinate system. It is important to note that the hand-eye relationship changes when the optical settings of the lens vary due to the movement of the front nodal point of the lens. Therefore, as the optical settings vary, the distances from the front nodal point of the lens to the object, referred to in the resolution and field of view planning sections, are expressed with respect to different front nodal points of the programmable lens. In order to avoid hand-eye calibration at various optical settings, offsets are computed during lens calibration between the front nodal point for which the hand-eye relationship has been calibrated and the front nodal point of the lens at any other optical setting. In this way, when distance D from the object to the front nodal point of the lens is computed from the resolution and field of view planning, $D - offset$ is used when placing the camera with the robot manipulator, where the offset is that associated with the chosen optical settings.

1.5.3 Experimental Results

Experimental results are shown in this section that demonstrate the effectiveness of the sensor planning method by finding zoom and focus settings of the programmable lens as well as camera to object distances so that visiblity, field of view and a specified resolution are all satisfied for a chosen target feature. The camera is then placed at the planned location with a robot manipulator, while the programmable lens is set to the computed values. The camera image is then observed to verify that the requirements are actually met.

1.5.3.1 Visibility Results

The visibility regions for the object and target of Figure 15 are first generated by the visibility algorithm. The occluded region of the top face F_{top} is shown in Figure 16, while the occluded region of the object as a whole is shown in Figure 17. The complement

of the occluded region consists of visibility envelopes that correspond to viewing the target through the small hole SH and the large hole LH of the object (Figure 15).

1.5.3.2 Resolution and Field of View Results for a variable intrinsic focal length lens.

We choose the feature of interest to be the width of the target T shown as L in Figure 15. where $L = 1$ in . The resolution limit is taken to be 3 pixels per 0.01 inches specified in the image frame buffer. For this resolution limit, two viewpoints are found that *just* satisfy this resolution, that is, each image pixel spacing corresponds to exactly 1/300 inches in object space, and thus the whole 1 inch width of the target projects to 300 pixels.

From (3b). the magnification ratio d/D is bounded from below by the resolution limit:

$$\frac{d}{D} \geq \frac{w}{l} \tag{9}$$

where

$$\frac{w}{l} = \frac{3 \times 23 \times 0.70642}{0.01 \times 25.4 \times 1000} = 0.192 \tag{10}$$

with $w = 3$ pixels and $l = 0.01$ inches, while using 0.70642 as the horizontal scale factor and 23 microns as the sensor element spacing in the horizontal direction. Based on the programmable lens calibration results shown in Figure 11 and Figure 12 , two viewpoints and their associated zoom and focus settings are selected that satisfy this resolution requirement in the limit, that is, (9) is close to an equality. These viewpoints are associated with points Λ and B on the $d/D = 0.192$ contour of Figure 18 and have the following parameter values:

zoom = 98	focus = 131	$d/D \simeq 0.192$	$D = 25.98$ in	offset = 11.48 in
zoom = 102	focus = 89	$d/D \simeq 0.192$	$D = 26.74$ in	offset = 11.84 in

The above zoom and focus values are the raw numbers returned by the lens controller. Their meaning is such that as the zoom units increase, the zoom lens "zooms-in" (i.e greater magnification, smaller field of view), while with increasing focus values the zoom lens focuses closer (i.e. at smaller object distances). Therefore, in the first camera setting, the lens is situated and focused closer (25.98-11.48 = 14.5 inches away from the feature), while in the second setting the camera is positioned and focused farther (at 26.74-11.84 = 14.9 inches), but the lens is "zoomed in" further.

These two camera locations are shown in Figure 17 as viewpoints Λ and B. Figure 14 shows the manipulator placed at viewpoint Λ and oriented towards the feature midpoint. The associated scenes of the target from these viewpoints are shown in Figure 20 and Figure 21 . These figures contain an engraved steel ruler with graduations of 0.1 and 0.01 of an inch so that the resolution can be verified. The three small bright line segments in these images are 6 pixels in the frame buffer and can be seen on the ruler to correspond to 0.02 inches at the far right, in the middle and at the far left of the feature. This validates that the resolution requirement of 3 pixels/0.01 inch is indeed satisfied.

On the other hand, the field of view constraint poses an upper limit on the magnification ratio d/D that can be achieved according to (7c).

$$\frac{d}{D} \leq \frac{l_{min}}{L} \tag{11}$$

where

$$\frac{I_{min}}{L} = \frac{512 \times 23 \times 0.70642}{25.4 \times 1000} = 0.327 \tag{12}$$

with $L = 1$ inch, and I_{min} is equal to a maximum number of 512 pixels in the horizontal direction, while using 0.70642 as the horizontal scale factor and 23 microns as the sensor element spacing in the horizontal direction.

Based on the programmable lens calibration results of (5a) and (5b) shown in Figure 11 and Figure 12, a viewpoint and its associated zoom and focus settings are selected that *just* satisfy this field of view limit, that is, (11) is close to an equality. This viewpoint lies outside the contour plot shown in Figure 18, but has the following parameter values:

$$zoom = 108 \quad focus = 95 \quad d/D = 0.295 \quad D = 21 \text{ in} \quad offset = 6.35 \text{ in}$$

This camera location is shown in Figure 17 as viewpoint C. The associated scene of the target from this viewpoint is shown in Figure 22. The bright line segment in this image is 460 pixels and can be seen to almost fill the image frame buffer in the horizontal direction.

Combining these resolution and field of view results, it is true that the points in the domain of feasible zoom and focus settings of the programmable lens, as well as those inside the band between the $d/D = 0.192$ and $d/D = 0.327$ contours (see Figure 18), define the contour region that satisfies both the resolution and field of view constraints. From Figure 12, this contour region determines a range of admissible (with respect to resolution and field of view) values of D. The minimum and maximum values of D in this range define a circular ring that can be intersected with the visibility regions and thus determine the region in three-dimensional space that satisfies *all three constraints*.

1.5.3.3 Resolution and Field of View Results for a constant intrinsic focal length lens.

Choosing the same resolution and field of view limits as in the case of a lens with variable intrinsic focal length, discussed in the previous section, we have from (10) and (12):

$$\frac{w}{l} = 0.192$$

$$\frac{I_{min}}{L} = 0.327$$

If the intrinsic focal length of the lens is 5 *in*, the upper and lower bounds for D can be computed from (4a) and (8a) as follows:

$$D = (1 + \frac{l}{w})f = (1 + 1/0.192) \times 5 = 31.04 \text{ in}$$

$$D = (1 + \frac{L}{I_{min}})f = (1 + 1/0.327) \times 5 = 20.29 \text{ in}$$

A viewpoint can now chosen inside the visibility regions at a distance D away from the target, where D is chosen between these two bounds, while the image distance can be easily computed from the Gaussian lens law. These minimum and maximum values of D thus define a circular ring that can be intersected with the visibility regions in order to determine the region in three-dimensional space that satisfies *all three constraints*.

These resolution and and field of view planning results for the constant intrinsic focal length lens can also be demonstrated for the case of the programmable lens by limiting the domain of zoom and focus settings to only those that generate a focal length of 5 in ($f = 5$ *in* contour in Figure 19). The points along this $f = 5$ *in* contour and between the

$d/D = 0.192$ and $d/D = 0.327$ contours (the whole $f = 5$ in contour in this case) define the contour segment that satisfies both the resolution and field of view constraints. From Figure 19, this contour segment thus determines the range of admissible (with respect to resolution and field of view) zoom and focus settings.

1.6 Conclusion

A new method and system for planning of camera placement and optical settings are presented that avoids occlusion and truncation of a chosen visual target while imaging this target so that a given resolution limit is satisfied. The method generates regions in space from where the target is visible, and computes admissible optical settings and camera to object distances for non-truncation and resolution satisfaction. Experimental results are shown placing a camera in a hand-eye configuration at planned locations and setting the zoom and focus controls of a programmable lens at planned values. The corresponding camera images are then observed to verify that the requirements are met.

The next step in this work is to determine the three-dimensional regions that satisfy the resolution and field of view constraints in a general viewing situation, as well as including additional sensor constraints, such as depth of focus. The need for other such planning functions will motivate future work and will result in more intelligent and autonomous machine vision applications for the future.

1.7 References

1. Cowan C., and Kovesi P., 1987, Automatic Sensor Placement from Vision Task Requirements, *SRI report*, Menlo Park, CA, June 1987.

2. Sakane S., Sato T., and Kakikura M., 1987, Model-Based Planning of Visual Sensors Using a Hand-Eye Action Simulator System: Heaven, *Electrotechnical Laboratory report*, MITI, Japan, 1987.

3. Tsai, R. Y., and Tarabanis, K., 1989, Occlusion-Free Sensor Placement Planning, *Proceedings of Third Annual Machine Vision Workshop*, New Brunswick, NJ, April 3-4, 1989.

4. Tarabanis K., and Tsai R.Y., 1989, Viewpoint Planning: the Visibility Constraint, *Proceedings of DARPA Image Understanding Workshop*, Palo Alto, CA, May 22, 1989.

5. Dietrich W., Nackman L.R., Sundaresan C.J., Gracer F., 1988, TGMS: An Object-Oriented System for Programming Geometry, *IBM Research Report*, IBM T.J. Watson Research Center, Yorktown Heights, NY, January 1988.

6. Wesley M. A., Lozano-Perez T., Lieberman L. I., Lavin M. A., Grossman D. D., A Geometric Modeling System for Automated Mechanical Assembly, *IBM Journal of Research and Development*, January 1980.

7. Preparata, F., and Shamos M., *Computational Geometry*, Springer Verlag, 1985.

8. Lenz, R. and Tsai, R., 1987, Techniques for Calibration of the Scale Factor and Image Center for High Accuracy 3D Machine Vision Metrology, *Proceedings of IEEE International Conference on Robotic and Automation*, Raleigh, NC.

9. Tsai, R., 1987, A Versatile Camera Calibration Technique for High Accuracy 3D Machine Vision Metrology using Off-the-Shelf TV Cameras and Lenses, IEEE Journal of Robotics and Automation, Vol. RA-3, No. 4, August.

10. Tsai, R. Y., and Lenz, R., 1988B, Real Time Versatile Robotics Hand/Eye Calibration using 3D Machine Vision, *International Conference on Robotics and Automation*, Philadelphia, PA, April 24-29.

11. Hansen C., and Henderson T., 1988, Toward the Automatic Generation of Recognition Strategies, *International Conference on Robotics and Automation*, Philadelphia, PA, April 24-29.

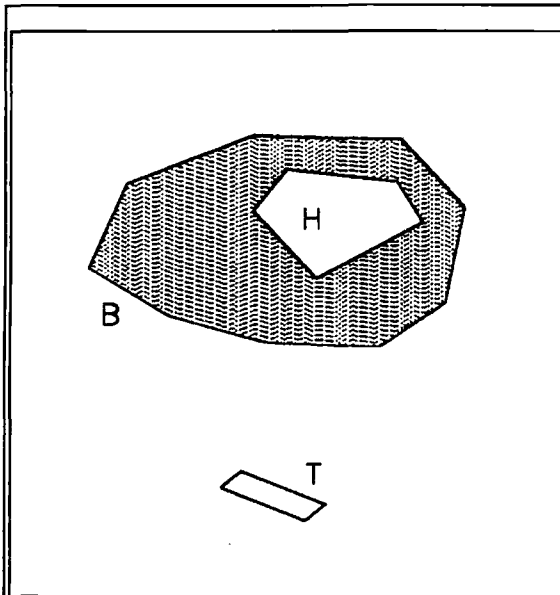12. Krotkov E.P., 1986, Focusing, *Technical Report MS-CIS-86-22*, University of Pennsylvania.

Figure 1. The occluding object is a polygon with a hole in it.
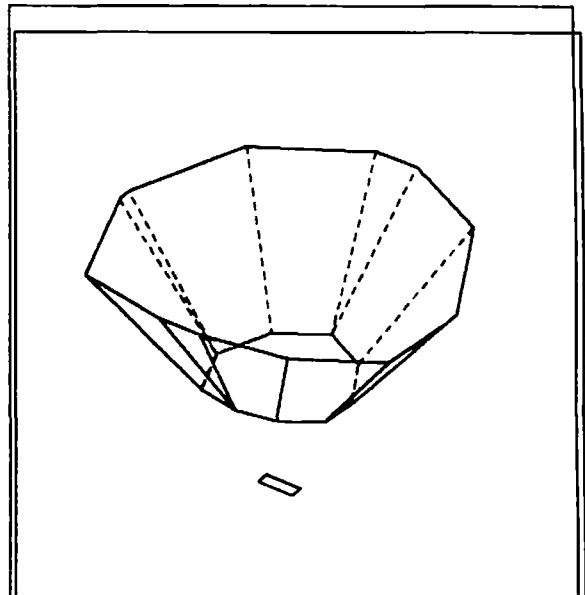
Figure 2. The computed occluded region of B.
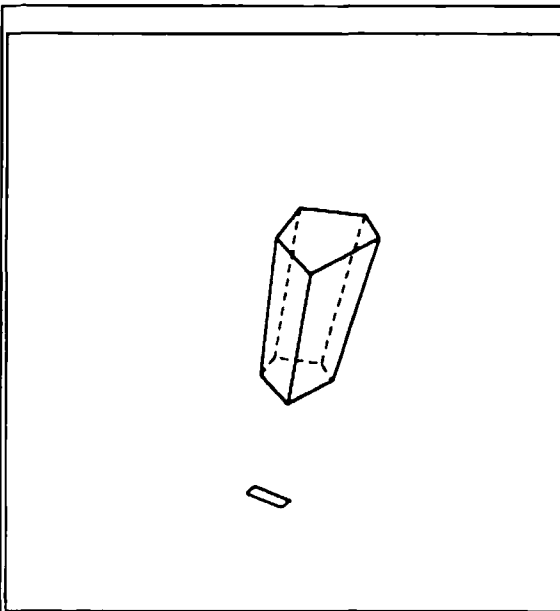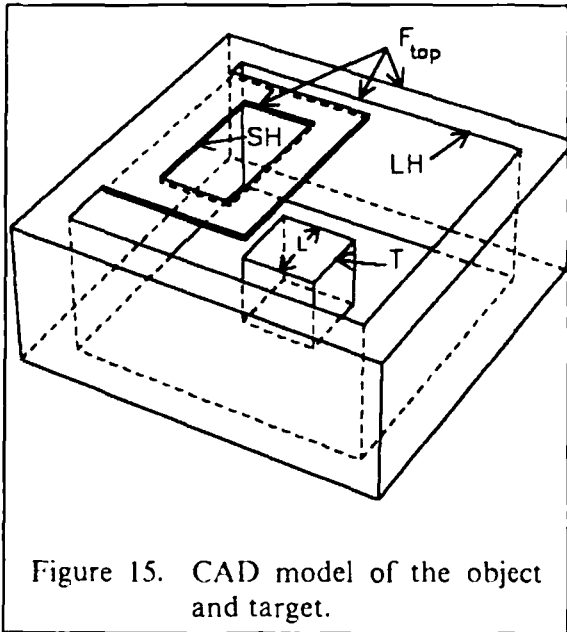

Figure 3. Viewing region for H.
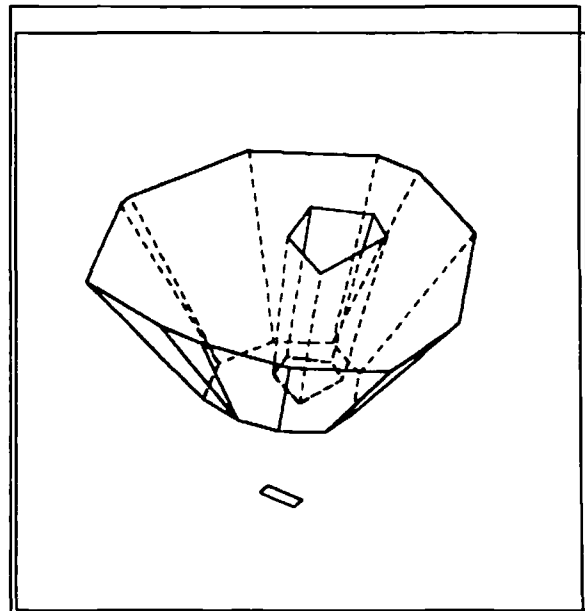
Figure 4. The resultant occluded region.

13
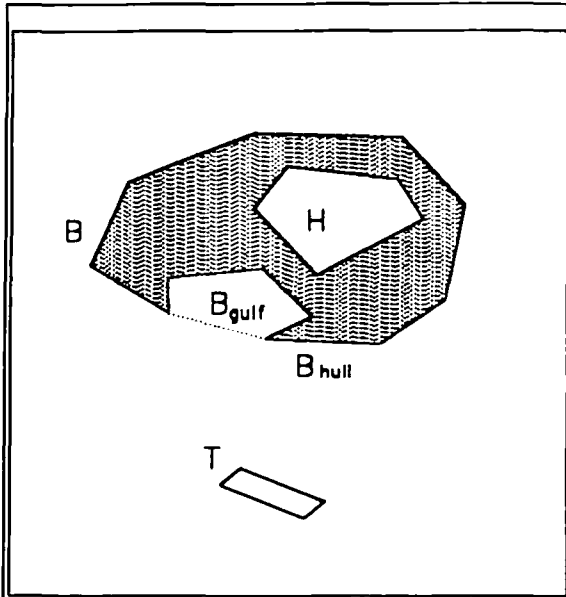
Figure 5. The occluding object is a concave polygon with a hole in it.
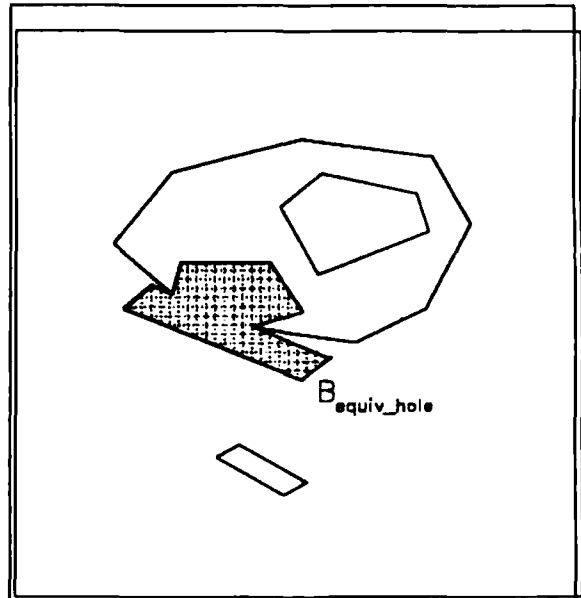
Figure 6. The gulf is extended to become a virtual gulf or equivalent hole.
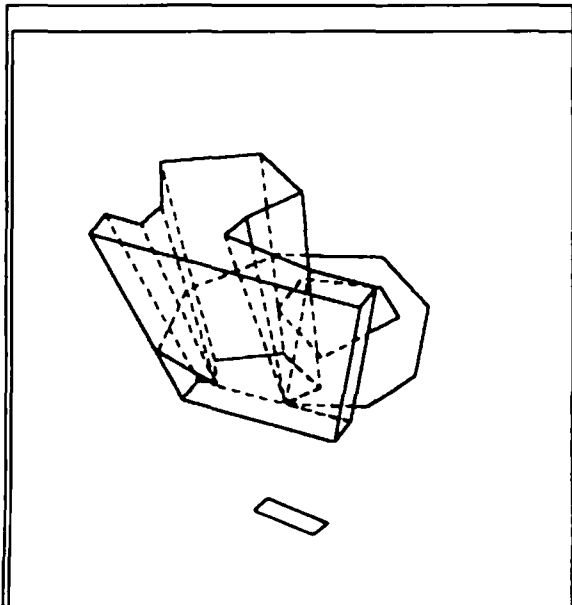
Figure 7. The viewing region through the equivalent hole.
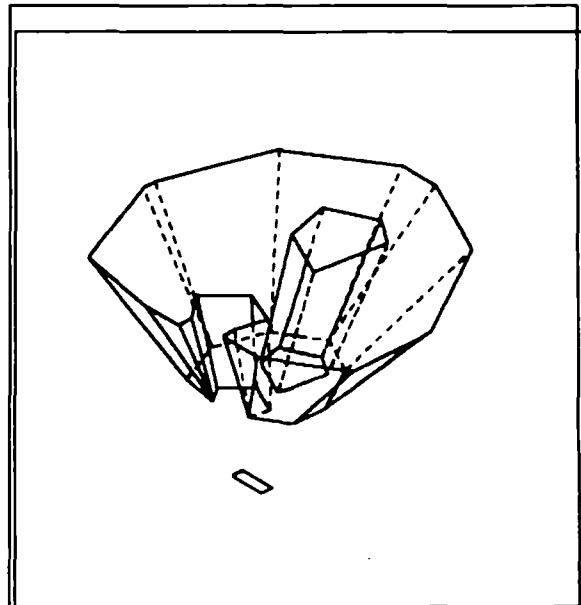
Figure 8. The resultant occluded region.

Figure 9.   The resolution constraint.

Figure 10.   The   field   of   view constraint.

MAGNIFICATION RATIO d/D

Figure 11.   The magnification ratio d/D for the zoom lens as a function of the zoom and focus settings.

OBJECT DISTANCE vs. ZOOM and FOCUS SETTINGS

Figure 12. The object to camera distance D for the zoom lens as a function of the zoom and focus settings.

Figure 13. The actual object and target.

Figure 14. The experimental setup.

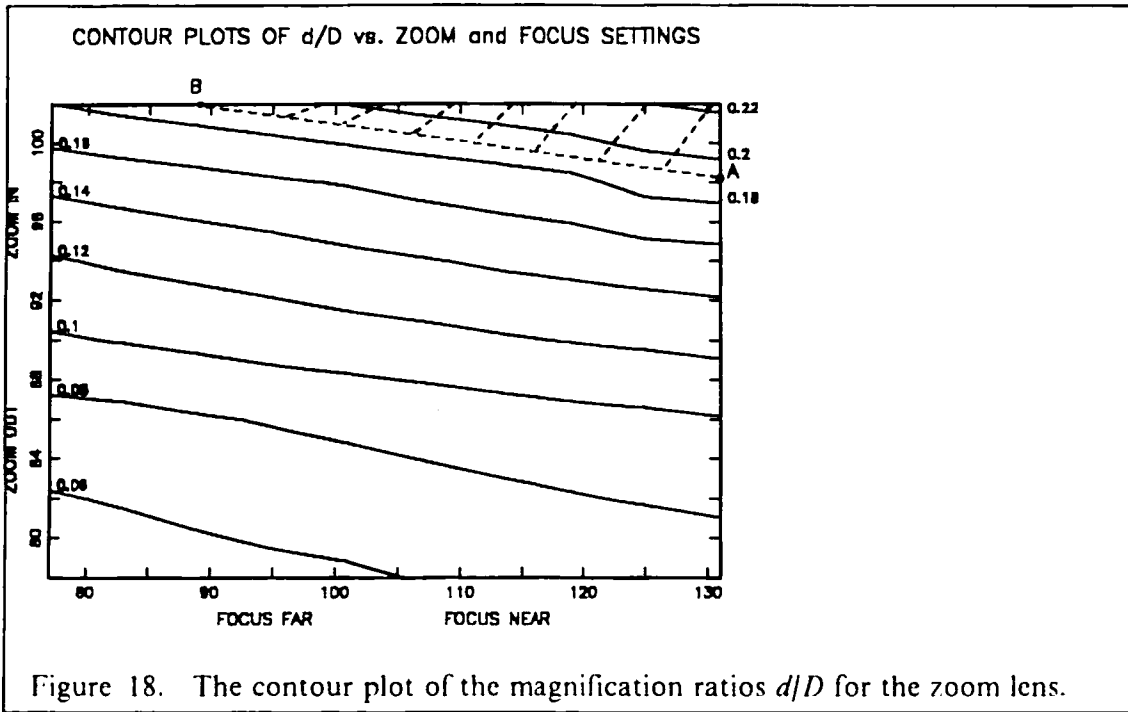Figure 15. CAD model of the object and target.
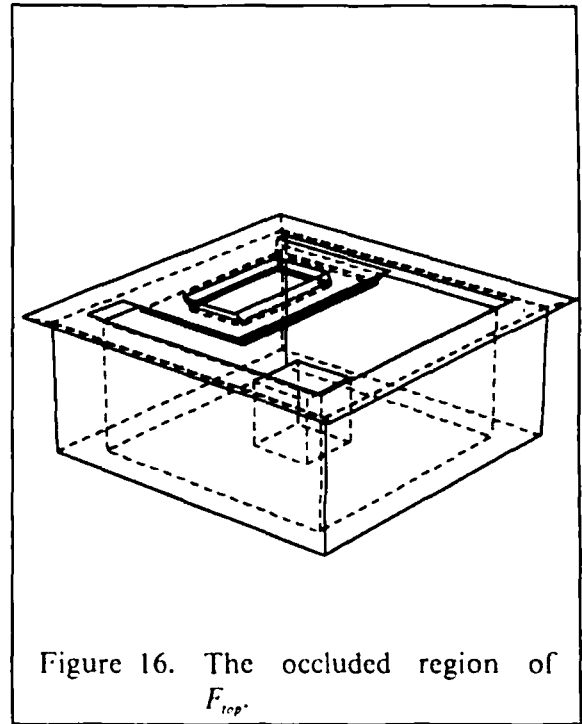
Figure 16. The occluded region of F_{top}.
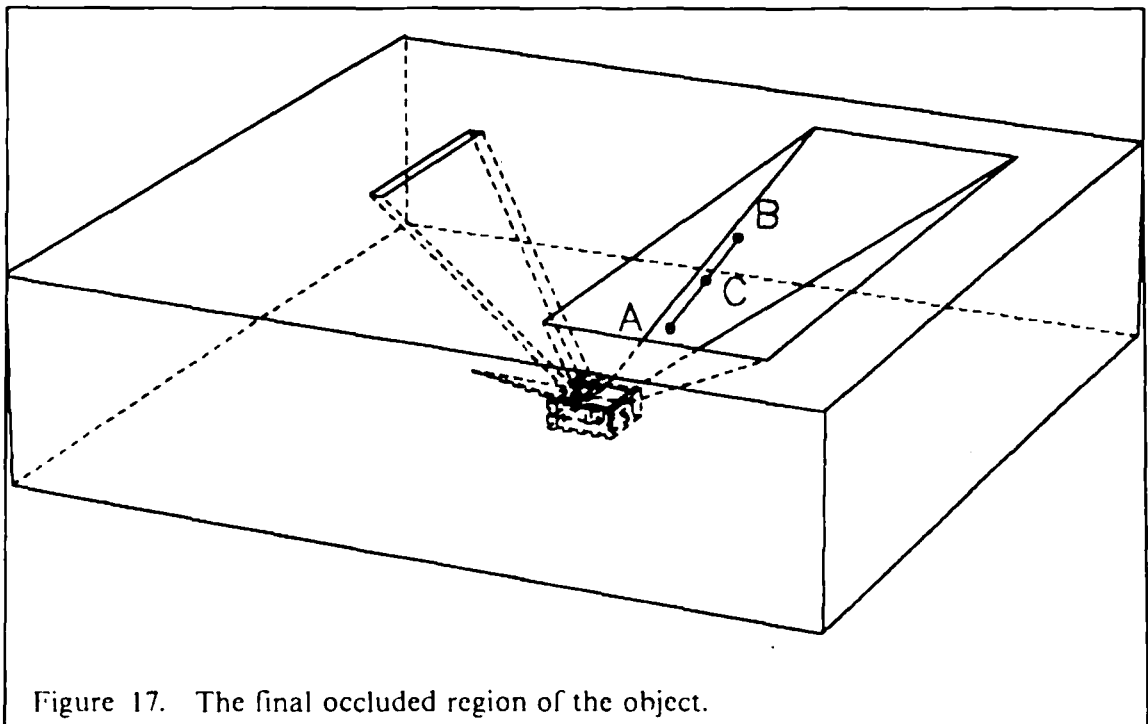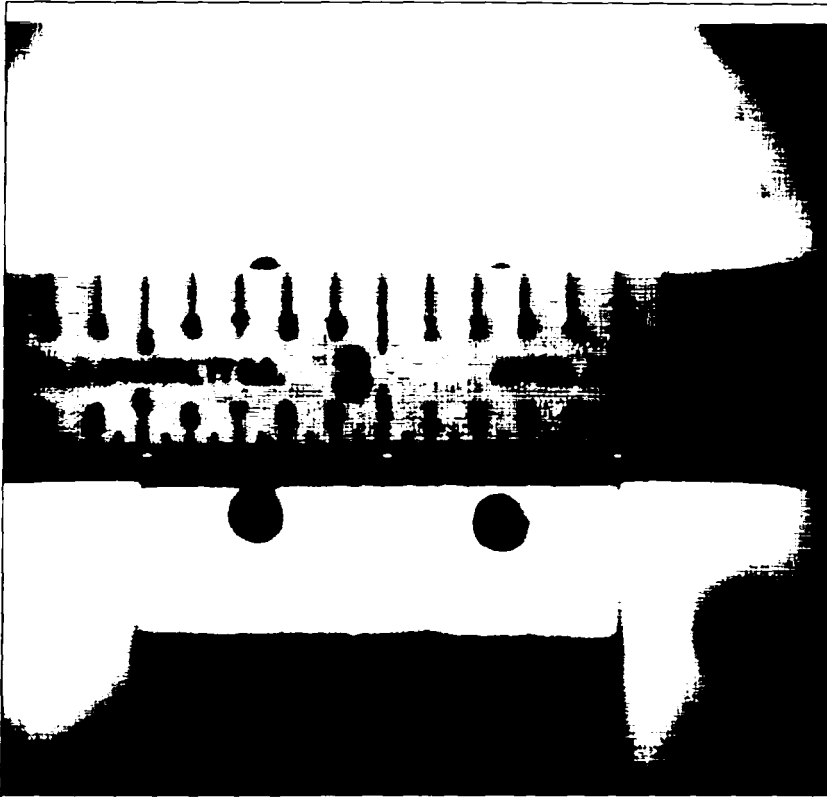

Figure 17. The final occluded region of the object.

Figure 18. The contour plot of the magnification ratios d/D for the zoom lens.

Figure 19. Contour plots of the magnification ratios d/D (solid lines) and the intrinsic focal lengths f (dashed lines).
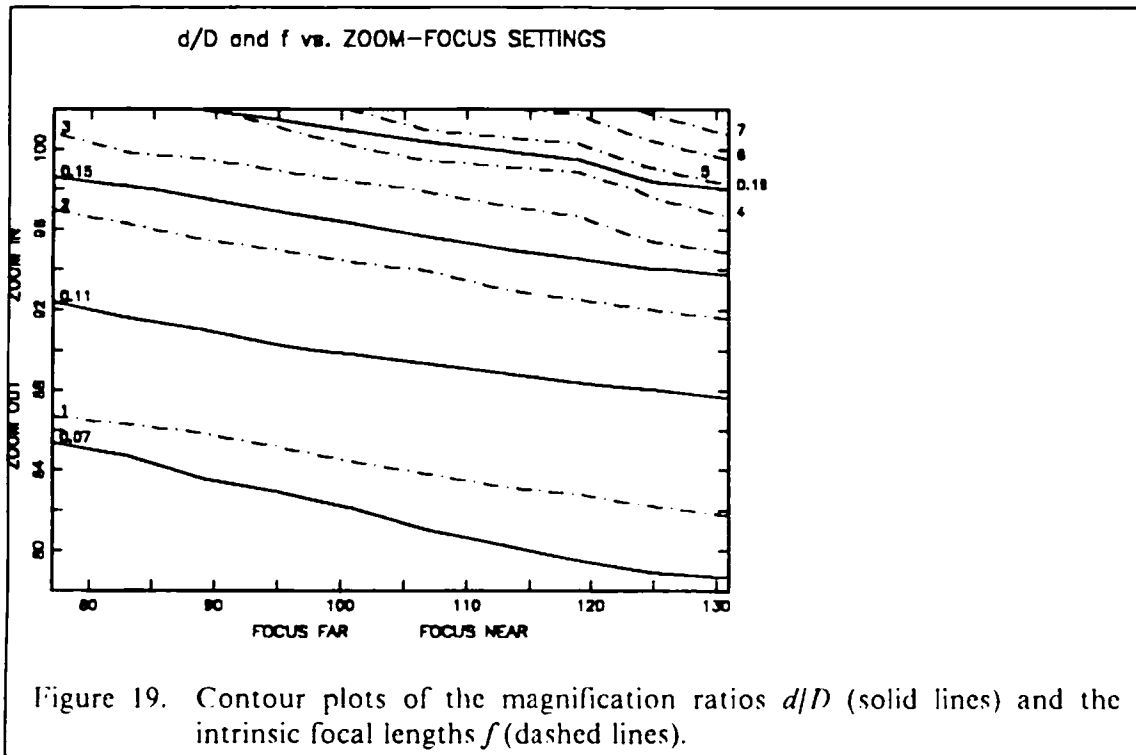
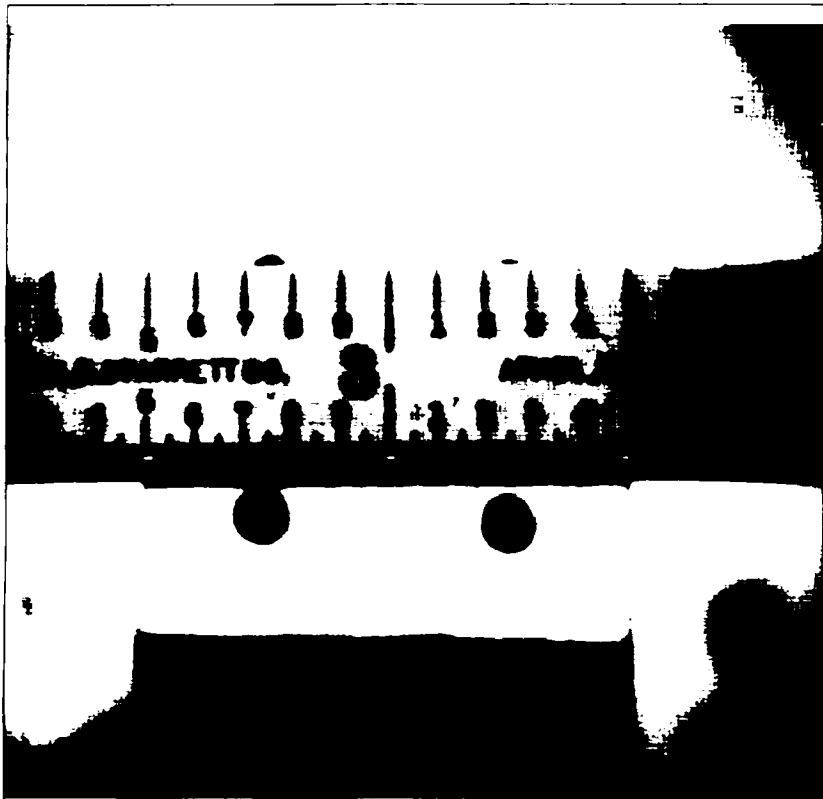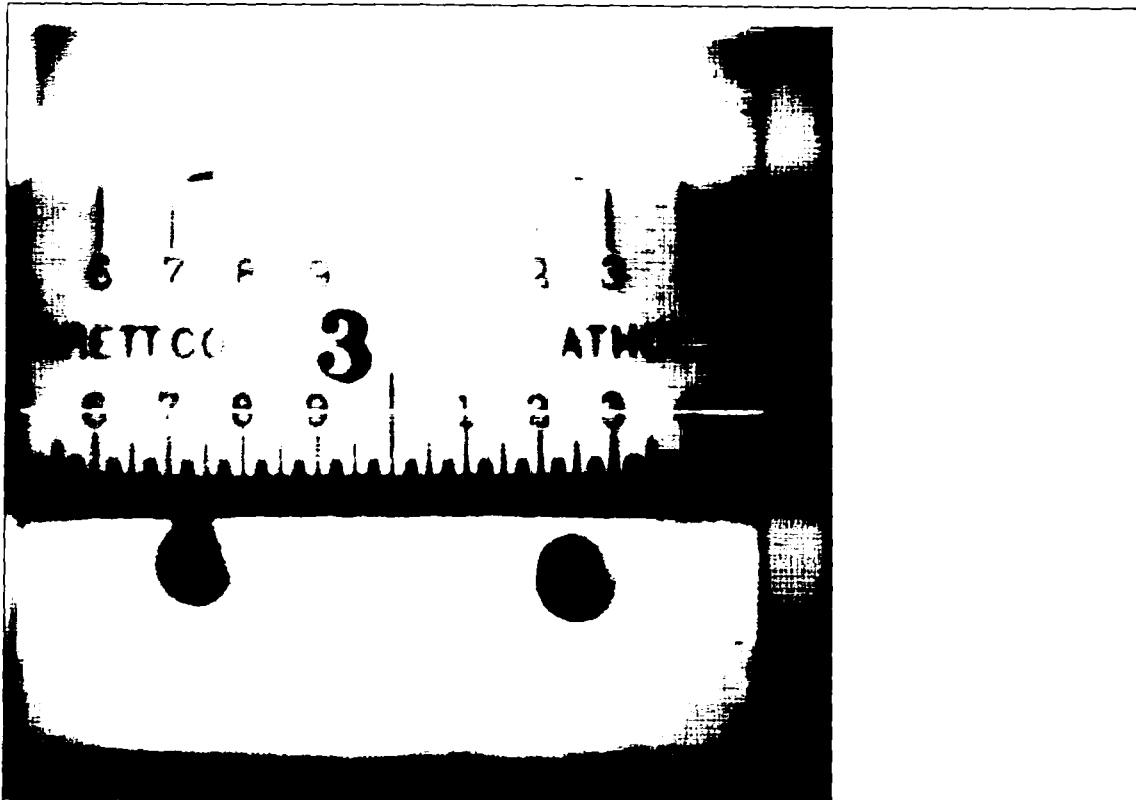Figure 20. The view of the target from viewpoint A.

Figure 21. The view of the target from viewpoint B.

Figure 22. The view of the target from viewpoint C.